

## Technical Note

## 3D Volume-Selective Turbo Spin Echo for Carotid Artery Wall Imaging With Navigator Detection of Swallowing

Lindsey A. Crowe, PhD,<sup>1\*</sup> Jennifer Keegan, PhD,<sup>1</sup> Peter D. Gatehouse, PhD,<sup>1</sup>  
Raad H. Mohiaddin, MD, PhD,<sup>1</sup> Anitha Varghese, MRCP, BSc,<sup>1</sup>  
Karen Symmonds, DCR(R),<sup>1</sup> Timothy M. Cannell, BApSc,<sup>1</sup> Guang Zhong Yang, PhD,<sup>2</sup> and  
David N. Firmin, PhD<sup>1</sup>

**Purpose:** To improve 3D volume-selective turbo spin echo (TSE) carotid artery wall imaging by incorporating navigators to reduce artifacts caused by swallowing.

**Materials and Methods:** Images were acquired on a Siemens Magnetom Sonata 1.5T scanner. 3D volume-selective TSE scans of the carotid arteries were acquired in six healthy volunteers. A cross-pair navigator placed on the back of the tongue was used to detect swallowing and movement. Two swallowing patterns were tested: 1) a single swallow approximately halfway through the scan time, at the center of  $k_z$ , and 2) repeated swallowing as often as possible throughout the scan period. Images were acquired with and without navigators for comparison. Signal intensity in the lumen was quantified for the quality of blood suppression, and the clarity of the vessel wall in the common carotid was ranked by four independent blinded observers.

**Results:** In general, lower signal intensity was recorded in the lumen, and decreased blurring and ghosting were observed on scans with navigator control. This reduction in lumen signal intensity signifies an improvement in the black-blood imaging technique. The differences likely reflect the improved double inversion/blood suppression efficiency due to cycles being rejected when the heart rate changed at the point of swallowing, or decreased motional blurring/ghosting of tissue when the navigator is used, or a combination of these two effects. A statistical analysis of image quality showed a significant difference between navigated and non-navigated scans as scored by four indepen-

dent, blinded observers. For both swallowing patterns, the mean score for the navigator images was on average 0.6 greater than that of non-navigator images (on a scoring scale of 0–5, where 0 = no vessel visible, and 5 = good delineation and blood suppression) and *P*-values for all observers were less than 0.01. Overall, the central swallow scans were scored higher than the repeated swallow scans. One reason for this may be the fact that the heart rate increased on swallowing, and this often lasted for one or two cardiac cycles after the navigator returned to the normal acceptance position. The effect of the increased heart rate after swallowing is likely to have an effect on double inversion blood suppression efficiency. Therefore, the increased amount of heart rate changes with repeated swallowing may have a greater adverse effect, even if the navigator rejects data views during the swallowing motion.

**Conclusion:** The clarity of vessel wall delineation and the apparent efficiency of blood suppression are reduced by swallowing during acquisition. Both motion blurring and quality of blood suppression are factors that can be improved with the use of a navigator accept/reject method.

**Key Words:** volume-selective imaging; black-blood MR; swallowing; navigator correction; carotid artery  
**J. Magn. Reson. Imaging 2005;22:583–588.**  
© 2005 Wiley-Liss, Inc.

ATHEROSCLEROTIC CAROTID ARTERY DISEASE is the most common cause of stroke and accounts for a substantial number of deaths and disabilities in the western world (1,2). A number of magnetic resonance (MR) methods have been described for vessel wall imaging. One of the main purposes of vessel wall imaging is to characterize plaque. However, the multiple contrasts (3) and high-resolution imaging required often lead to increased imaging times. A method to improve image quality and avoid the need for repeat scans is therefore important.

Significant work on characterizing plaque by MR has been reported by several groups, with two-dimensional (2D) turbo spin echo (TSE) sequences being used in clinical applications (4–10). Carotid artery disease is

<sup>1</sup>Magnetic Resonance Unit, Imperial College and Royal Brompton Hospital, London, UK.

<sup>2</sup>Royal Society/Wolfson MIC Laboratory, Imperial College, London, UK. Contract grant sponsors: British Heart Foundation; HEFCE; CORDA the Heart Charity.

Presented in part at the 12th Annual Meeting of ISMRM, Kyoto, Japan, 2004. Abstract 1900.

\*Address reprint requests to: D.F., Magnetic Resonance Unit, Imperial College, Royal Brompton and Harefield NHS Trust, Sydney Street, London, SW3 6NP, UK. E-mail: D.Firmin@ic.ac.uk

Received June 28, 2004; Accepted July 13, 2005.

DOI 10.1002/jmri.20424

Published online 13 September 2005 in Wiley InterScience (www.interscience.wiley.com).

known to be a good marker for other vessel disease because the carotid artery is a common location for atherosclerosis. Superficial vessels enable the use of surface coils for higher SNR. Since stabilization of the head is a relatively simple procedure, the vessel is generally straight, and respiratory motion is minimal, the carotid artery is often the artery of choice for studies of atherosclerosis. Most of these studies involve 2D imaging; however, in vivo coronary vessel wall imaging using a three-dimensional (3D) spiral acquisition has also been reported (11,12). This approach uses a nonselective inversion prepulse and a 2D selective local inversion prepulse to suppress unwanted signal outside the volume of interest.

As these MR arterial wall imaging methods become more widely available clinically, it is becoming more important to optimize the techniques used. We recently developed a 3D volume-selective TSE sequence for arterial wall imaging (13). The primary advantage of this sequence is that it enables greater coverage of the volume of interest in the same amount of time as the equivalent 2D method, while maintaining the same signal-to-noise ratio (SNR), due to the significantly smaller phase-encode field of view (FOV). In 3D volume-selective TSE scans of carotid arteries in some patients, blurred images have been observed that may be attributed to swallowing/throat motion during the scan. Artifacts may be caused by motion of the vessel and/or surrounding tissue, or by the change in blood flow patterns caused by the increased heart rate on swallowing. This also has an adverse effect on the timing of the double inversion in relation to the changes in heart rate. Similar effects have been observed in other carotid MRI techniques (14). Images are acquired during free breathing over several minutes, which means that swallowing is likely to occur during the acquisition. Another limitation of the 3D approach is the increased difficulty of suppressing blood signal. This problem and methods to reduce it were addressed in another study (15). The purpose of the present study was to observe the effect of swallowing motion and investigate the possibility of removing its associated artifacts during vessel wall imaging of the carotid arteries.

## MATERIALS AND METHODS

All scans were performed on a Siemens Magnetom Sonata 1.5 T scanner. A 3D volume-selective TSE sequence was used to image the carotid arterial wall, with the slab centered on the carotid bifurcation (13). Navigator and accept/reject algorithms were incorporated into the MR sequences to assess the effects of any swallowing motion.

For the volume-selective TSE images, the FOV used was  $120 \times 24$  mm and imaging matrix size was  $256 \times 52$ , giving a true pixel size of  $0.47 \text{ mm} \times 0.47 \text{ mm}$  (which is further interpolated by a factor of 2 during reconstruction) with 18 slices (true slice thickness = 2 mm) and 40% slice oversampling to avoid signal wrap. Volume excitation is achieved by switching the slice-selection gradient of the  $90^\circ$  excitation pulse onto the phase-encoding axis and scaling its thickness to the phase FOV. This is followed by the  $180^\circ$  refocusing

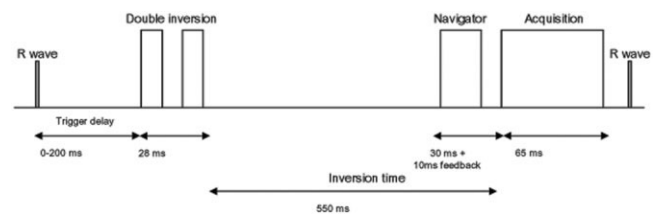


**Figure 1.** Schematic of sequence elements.

pulse. Dark-blood, double-inversion preparation was applied to all TSE images. An echo train length of 11 and a bandwidth of 43.5 kHz were used to fit the scan within the desired acquisition window (65 msec) to avoid motion blurring due to pulsatility. For these  $T_1$ -weighted images, the sequence was triggered on every cardiac cycle with a short echo time (TE) of 11 msec. Each scan lasted one to two minutes, depending on the heart rate and navigator acceptance efficiency. Within the cardiac cycle a trigger delay can be used to place the acquisition in diastole, and the inversion time was fixed appropriately to the RR interval of the subject. A black-blood double inversion technique was used with an inversion time of 550 msec, which in most cases placed the acquisition window into diastole. This inversion time was longer than would be expected theoretically. It was found in earlier studies that this longer inversion time gave better results, possibly because of the longer time it afforded for reinverted blood in the 3D imaging slab to be replaced (13). If a subject's heart rate was particularly slow, a delay of up to 200 msec was added before the double inversion preparation. If the heart rate was fast, the inversion time was decreased to maintain cardiac gating on every cycle. The dark-blood preparation consisted of a nonselective inversion and slice-selective reinversion with a thickness 1.2 times that of the full 3D imaging slab. The sequence timings are illustrated in Fig. 1.

The images were acquired using a purpose-built, two-element, phased-array coil (Machnet BV, The Netherlands). The coil was placed on the side of the neck with the elements in posterior–anterior alignment. These elements cover a single side and can be used in combination with a second two-element coil to image both sides of the neck simultaneously. A single side of the carotid arteries was imaged for this study to ensure perpendicular location of the vessels and centering on the bifurcation. Localization of the bifurcation was achieved with a transverse 2D multislice time-of-flight (TOF) scan of the entire length of artery covered by the coil (~12 cm) with a superior saturation band to suppress venous flow. A low-resolution 2D TSE scan, in the vessel plane, was located in the TOF images by using a three-point piloting tool and positioning markers in the center of the lumen above and below the bifurcation. This was then used to plan the 3D scan to ensure that slices were as perpendicular to the vessel as possible.

A cross-pair navigator placed on the back of the tongue was used to detect swallowing. This consists of slice-selective  $90^\circ$  and  $180^\circ$  excitations, the intersection of which is positioned over and perpendicular to the back of the tongue, forming a column of signal for a 1D

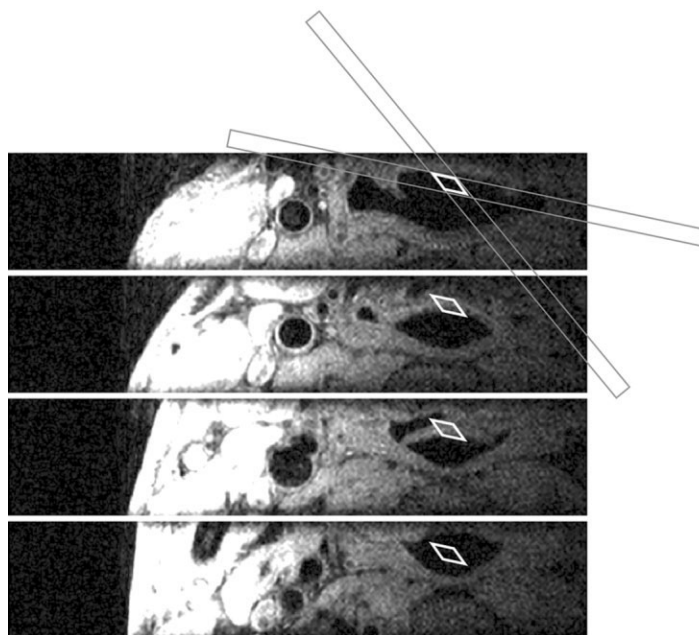


**Figure 2.** Images showing position of crossed pair navigator. The column navigator runs through perpendicular to the images shown, as indicated by the white boxes with the tongue coming into the column in the region of the central slices.

frequency encode. This column runs in a head-foot direction and detects an edge on the tongue that moves with swallowing. This edge is usually close to the carotid bifurcation, and sufficient signal is obtained from the carotid surface coil to detect the edge. The navigator was acquired in all scans, but in only half was used with an accept/reject algorithm. For the remainder it was used only to monitor the swallowing pattern. This had the advantage that the signal voids from the intersecting navigator planes were visible on all images, and thus blinding for the purposes of image comparison was not a problem. This also meant that any slight timing changes caused by the navigator were consistent in all scans.

Prospective navigator gating with a  $\pm 2$  mm acceptance window was used. This is illustrated in Figs. 2 and 3. Because of the long inversion time used, the navigator was acquired at the end of the double inversion preparation, just before the short FSE readout. This minimized the possibility of a change in tongue position between the navigator decision and the time of data acquisition, and yielded optimum signal intensity in the navigator output by allowing the signal to recover after the reinversion.

Two swallowing patterns were tested on both a navigator and a non-navigator acquisition. For the first test the subjects were asked to swallow halfway through the scan (this was expected to represent a worst-case single swallow). For the other tests the subjects were asked to swallow as often as possible. In the latter case this was about every 10–20 seconds during a two-minute scan.

The study population included six healthy subjects (average age = 35 years, range = 23–47 years), who provided informed consent. Images were analyzed using CMRTTools (Imperial College, London, UK).

It had previously been noted that swallowing during the 3D volume-selective acquisition generally degraded the whole of the imaging volume. Slices through the common carotid were used in this study so that other

problems such as recirculating flow that occur at the bifurcation would not further complicate the measurements.

Signal intensities within the lumen and wall, as well as the noise level, were quantified, and paired t-testing and Bland-Altman analysis were used to compare the differences between navigator and non-navigator scans. The images were also scored by four blinded

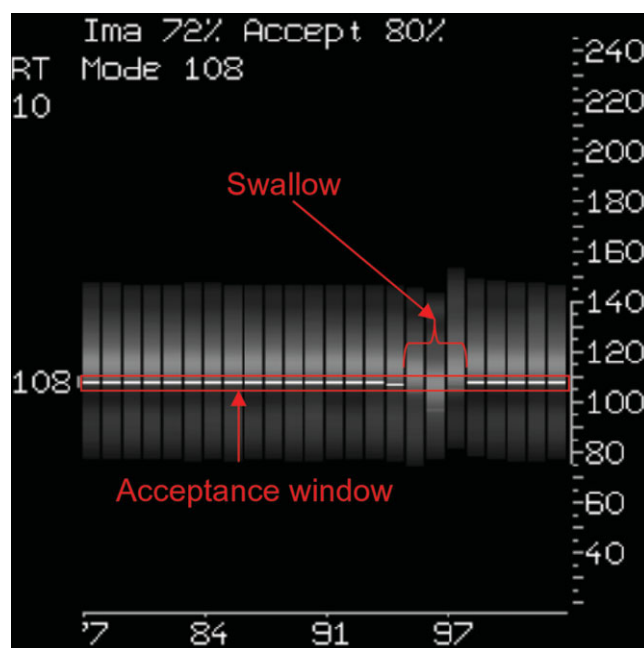


**Figure 3.** Navigator trace from a section of a scan during which the subject swallowed as often as possible. Each column represents a 1D reconstruction of the vertical navigator acquired each cardiac cycle immediately before the TSE readout. A solid white edge in the acceptance window shows data that have been accepted.

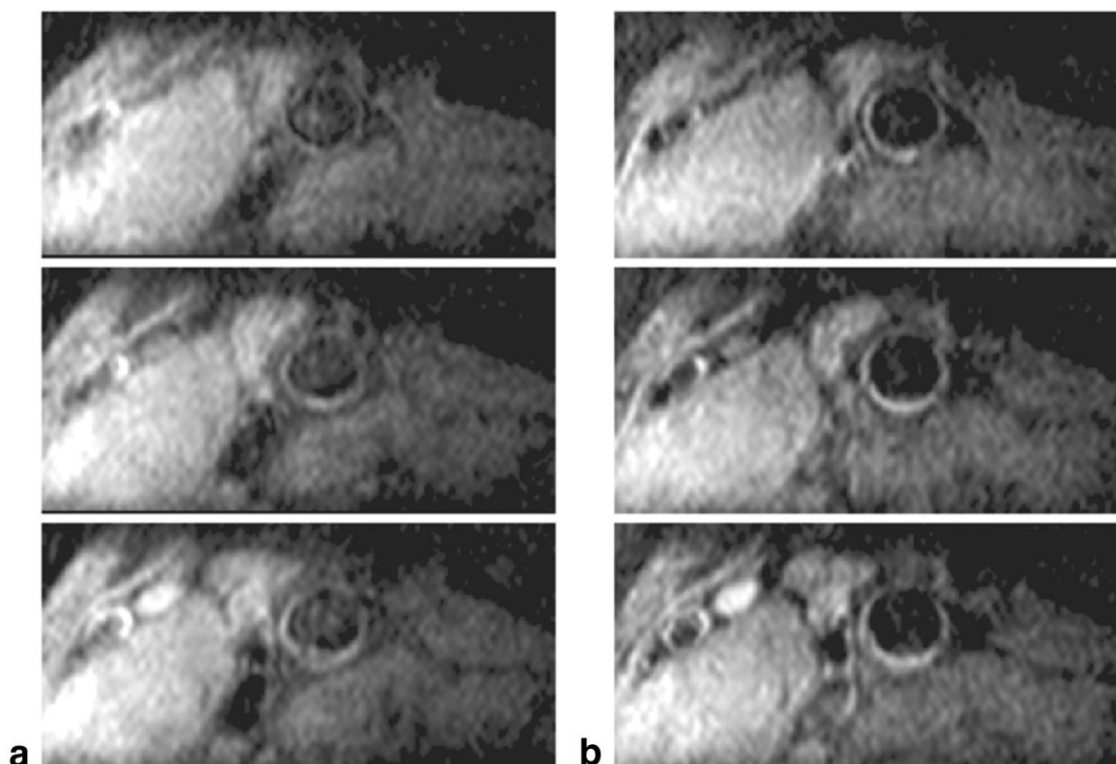


**Figure 4.** Comparison of image quality in the common carotid (single central swallow) with (a) no navigator control and (b) navigator control.

observers in terms of the clarity of the vessel wall. For the scoring, 11 slices in the common carotid and start of the bifurcation were graded on a scale of 0–5 (0 = no vessel visible; 5 = good delineation and blood suppression), taking into account visibility of the vessel, ghosting, clear delineation of the inner and outer extents of the wall, and lumen suppression. For each 3D scan a composite image quality score was calculated as the average of the image quality scores over the 11 contiguous slices. Paired Wilcoxon analyses were performed to compare the composite image quality scores between the navigator and non-navigator scans. Analyses were performed for both swallowing patterns (single central swallow and repeated swallowing) and for all four observers.

## RESULTS

Overall, the swallowing motion caused blurring and ghosting in the  $k_z$  (slice) and  $k_y$  (phase-encode) directions, leading to reduced image quality throughout the 3D slab. A comparison of three slices from a typical scan with a single central swallowing is shown in Fig. 4. The lumen and wall clarity are improved in the scan with navigator-controlled accept/reject (b) over the non-navigator-controlled images (a). Both the wall signal intensity and noise level remained unchanged between the navigator and non-navigator scans (both  $P = ns$ ), whereas the quality of the blood signal suppression (as measured by changes in the lumen signal intensity) improved ( $P < 0.02$ ; Table 1). The Bland-Altman plot (Fig. 5) shows that for all but one subject the navigator

scans resulted in a reduced lumen signal. For this subject (subject 2, gray points on Fig. 5) both the lumen and tissue signal intensity were low and the difference was unclear. This subject had poorer overall SNR due to coil positioning and generally poor lumen/tissue definition.

For all four observers, the image quality scores for the navigator images were approximately 0.6 greater than those for the non-navigator images (on a scoring scale of 0–5) for both swallowing patterns. Paired Wilcoxon analyses showed that the improvement in image quality with navigator gating was statistically significant for both the single central swallow scans ( $P < .05$  for all four observers) and those carried out during repeated swallowing ( $P < .05$  for all four observers). Figure 6 shows the mean of these scores for each observer. Apart from one pair, all navigator images were scored higher

Table 1  
Mean Difference in Lumen Signal Artifact With and Without Navigator Gating

Subject	Lumen signal intensity		
	No navigator	Navigator	%Difference
1	53.4	36.7	45.4
2	20.9	21.8	−4.4
3	73.8	59.6	23.9
4	71.2	45.9	55.1
5	36.3	27.2	33.4
6	34.8	29.5	17.9

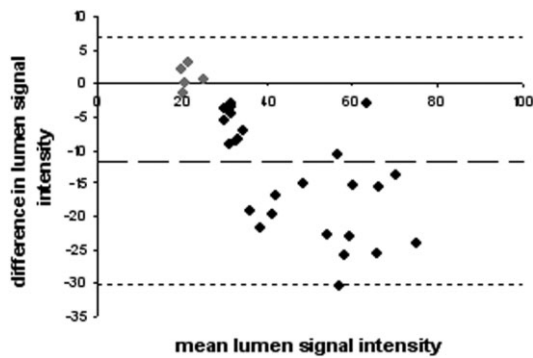


**Figure 5.** Bland-Altman plot of lumen signal intensity differences between navigator-controlled and non-navigator-controlled scans. Gray points represent subject 2, as explained in the text.

than the non-navigator scan on the same subject with the same swallowing instructions. The one exception is likely due to a poor choice of navigator position, since several lines were wrongly accepted during the swallowing motion as an alternative edge in the navigator trace came into the acceptance window. The subject with poor SNR and little difference in the quantitative measurement of lumen signal also had similar scores for navigator and non-navigator scans. In general, the central swallow scans were scored higher than the repeated swallow scans. The mean scores for each subject compared over all observers for the navigator control scans were  $3.1 (\pm 1.3)$  for the single swallow and  $2.7 (\pm 1.2)$  for repeated swallowing with a significant difference ( $P < 0.05, N = 6$ ). For non-navigator-controlled scans the scores were  $2.4 (\pm 1.0)$  and  $2.1 (\pm 1.2)$  ( $P < 0.05, N = 6$ ).

In terms of scan time, the central and repeated swallow scans had average ( $\pm$ SD) scan efficiencies, due to navigator accept/reject, of  $90\% (\pm 4\%)$  and  $70\% (\pm 9\%)$ , respectively. This scan efficiency represents the percentage of acquired data that is accepted by the navigator algorithm to form the final image. For example, a scan efficiency of 70% means that a 70-second scan with all data accepted would be extended to 100 seconds. The larger SD for the efficiency of the repeated swallow scans may have resulted from the different frequency of swallowing between subjects (five to 12 per scan).

**DISCUSSION**

There are two likely causes for the difference observed in lumen signal intensity: 1) poorer double inversion/blood suppression efficiency due to heart rate changes at the point of swallowing, and 2) increased motional blurring/ghosting of tissue in the lumen without rejection of data by the navigator control.

The k-space ordering used in the 3D sequence consisted of a reduced number of  $k_y$  steps due to the volume-selective method used. Once  $k_y$  was completed, the  $k_z$  slice encoding was incremented. The center of  $k_z$  was acquired at the center of the scan because we did not use asymmetric raw data coverage or partial-Fourier meth-

ods. For the navigator-gated scans, the efficiency was taken into consideration when the swallowing instructions were given. With this ordering, the centrally timed swallow, as tested, occurred at the center of k-space, and thus represented artifacts from the expected worst-case single swallow. Repeated swallowing was used as a deliberate test for the effect of swallowing.

In addition to motion artifacts, the effect of swallowing on blood flow patterns should also be considered. The increased heart rate on swallowing (16) often lasted for one or two cardiac cycles after the navigator returned to the normal accept position. The effect of this small percentage increase in heart rate after a swallow is likely to have an effect on the double inversion preparation and therefore blood suppression efficiency. The variable nature of these changes over a couple of cardiac cycles results in unpredictable effects on the suitability of the inversion time. Heart rate irregularity will also lead to varying  $T_1$  recovery, causing ghosting in all tissues. Repeated swallowing causes more heart rate changes during the scan, leading to reduced image quality even if the navigator rejects scans during the swallowing motion. A further improvement to this technique might be to use an additional arrhythmia rejection algorithm to exclude the additional short cycles that follow the swallow, or to incorporate a more intelligent algorithm to recalculate and adjust the double inversion time during the scan. Similar methods have been reported for real-time trigger delay adaptation (17).

Even with the subjects swallowing as often as possible, the worst-case acceptance rate for the navigator sequence was on average 70%, indicating the value of this technique as a standard “safety net” to help in the case of swallowing without interfering with the image acquisition or prolonging the scan time. This could be significantly helpful for scans that last several minutes, since in such scans a single movement can affect the quality of the whole slab and necessitate repeated data acquisitions.

In conclusion, the clarity of vessel wall delineation and the apparent efficiency of blood suppression are improved by dealing with swallowing motion and associated heart-rate irregularity. The image quality can be improved by using a navigator accept/reject method.

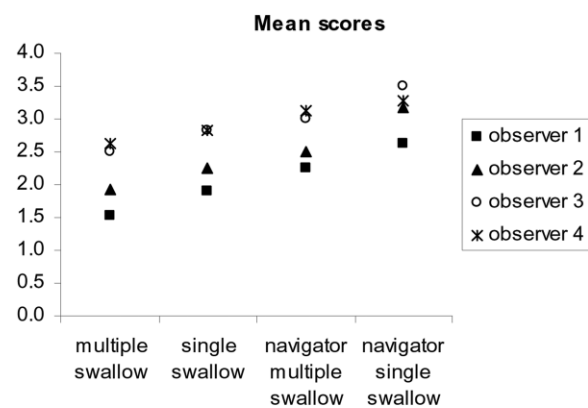


**Figure 6.** Mean score for each type of image for each observer.

## ACKNOWLEDGMENTS

We thank the staffs of the Royal Brompton Hospital CMR Unit, the Royal Society/Wolfson MIC Laboratory at Imperial College, and Siemens for their support.

## REFERENCES

1. Moneta GL, Taylor DC, Zierler RE, Kazmers A, Beach K, Strandness Jr DE. Asymptomatic high-grade internal carotid artery stenosis: is stratification according to risk factors or duplex spectral analysis possible? *J Vasc Surg* 1989;10:475–482.
2. Inzitari D, Eliasziw M, Gates P, et al. The causes and risk of stroke in patients with asymptomatic internal carotid-artery stenosis. North American Symptomatic Carotid Endarterectomy Trial Collaborators. *N Engl J Med* 2000;342:1693–1700.
3. Clarke SE, Hammond RR, Mitchell JR, Rutt BK. Quantitative assessment of carotid plaque composition using multicontrast MRI and registered histology. *Magn Reson Med* 2003;50:1199–1208.
4. Yuan C, Mitsumori LM, Beach KW, Maravilla KR. Carotid atherosclerotic plaque: noninvasive MR characterization and identification of vulnerable lesions. *Radiology* 2001;221:285–299.
5. Fayad ZA, Fuster V. Clinical imaging of the high-risk or vulnerable atherosclerotic plaque. *Circ Res* 2001;89:305–316.
6. Toussaint JF, LaMuraglia GM, Southern JF, Fuster V, Kantor HL. Magnetic resonance images lipid, fibrous, calcified, hemorrhagic, and thrombotic components of human atherosclerosis in vivo. *Circulation* 1996;94:932–938.
7. Corti R, Fayad ZA, Fuster V, et al. Effects of lipid lowering by simvastatin on human atherosclerotic lesions: a longitudinal study by high-resolution, noninvasive magnetic resonance imaging. *Circulation* 2001;104:249–252.
8. Corti R, Fuster V, Fayad ZA, et al. Lipid-lowering by simvastatin induces regression of human atherosclerotic lesions: two years' follow-up by high-resolution noninvasive magnetic resonance imaging. *Circulation* 2002;106:2884–2887.
9. Mohiaddin RH, Burman ED, Prasad SK, et al. Glagov remodeling of the atherosclerotic aorta demonstrated by cardiovascular magnetic resonance: the CODA asymptomatic subject plaque assessment research (CASPAR) project. *J Cardiovasc Magn Reson* 2004;6:517–525.
10. Jaffer FA, O'Donnell CJ, Larson MG, et al. Age and sex distribution of subclinical aortic atherosclerosis: a magnetic resonance imaging examination of the Framingham Heart Study. *Arterioscler Thromb Vasc Biol* 2002;22:849–854.
11. Botnar RM, Kim WY, Bornert P, Stuber M, Spuentrup E, Manning WJ. 3D coronary vessel wall imaging utilizing a local inversion technique with spiral image acquisition. *Magn Reson Med* 2001;46:848–854.
12. Kim WY, Stuber M, Bornert P, Kissinger KV, Manning WJ, Botnar RM. Three-dimensional black-blood cardiac magnetic resonance coronary vessel wall imaging detects positive arterial remodeling in patients with nonsignificant coronary artery disease. *Circulation* 2002;106:296–299.
13. Crowe LA, Gatehouse P, Yang GZ, et al. Volume-selective 3D turbo spin echo imaging for vascular wall imaging and distensibility measurement. *J Magn Reson Imaging* 2003;17:572–580.
14. Serfaty JM, Herigault G, Yuan C, Douek PC. Sources of carotid artery motion during carotid artery plaque imaging. In: Proceedings of the 15th Annual Meeting of the MR Angio Club, Dublin, Ireland, 2003.
15. Crowe LA, Mohiaddin RH, Varghese A, Yang GZ, Firmin DN. Identification and removal of residual signal from slow flowing blood in 3D volume-selective TSE arterial wall imaging using a velocity sensitive phase reconstruction method. In: Proceedings of the 12th Annual Meeting of ISMRM, Kyoto, 2004. Abstract 1901.
16. Sherozia OP, Ermishkin VV, Lukoshkova EV. Dynamics of swallowing-induced cardiac chronotropic responses in healthy subjects. *Bull Exp Biol Med* 2003;135:322–326.
17. Huber ME, Buehrer M, Kozerke S, Boesiger P. Real-time trigger delay adaption in coronary MRA. Poster Abstract 216 from Seventh Annual SCMR Scientific Sessions. *J Cardiovasc Magn Reson* 2004;6:103–126.